Special Issue on "Medicinal Chemistry"

J. Indian Chem. Soc.,
Vol. 97, August 2020, pp. 1227-1235

Design, synthesis and biological evaluation of novel DPP-IV inhibitors

Chirag Karelia, Kailash Parmar, Divya Teli and Mahesh Chhabria*

Department of Pharmaceutical Chemistry, L. M. College of Pharmacy, Navrangpura, Ahmedabad-380 009, Gujarat, India

E-mail: mahesh.chhabria@rediffmail.com

Manuscript received online 20 July 2020, accepted 01 August 2020

Diabetes mellitus is one of the top ten leading causes of death worldwide. DPP-IV inhibition became an attractive target in controlling type 2 diabetes. Because of the several adverse effects associated with current DPP-IV inhibitors, the discovery and development of newer DPP-IV inhibitors are crucial. Ligand-based 3D QSAR pharmacophore modeling method was used in recognizing the important molecular chemical features of potent DPP-IV inhibitors. The best pharmacophore model (Hypo 1) was generated using *HypoGen* algorithm of Discovery Studio 2.1 (DS). Based on the Hypo 1 model, four novel designed compounds were synthesized, characterized and screened for their DPP-IV inhibitory potentials. All the compounds **(9)**, **(10)**, **(11)** and **(12)** showed IC_{50} values ranging from 0.035–0.35 μM.

Keywords: Type 2 diabetes, DPP-IV inhibitor, 3D QSAR pharmacophore, virtual screening, *S*,*N*-acetal, *N*,*N*-acetal.

Introduction

Diabetes mellitus is a chronic metabolic disorder characterized by an elevated blood glucose level (hyperglycemia) caused by insulin deficiency, often combined with insulin resistance. The most common type is type 2 diabetes. Approximately, 463 million adults have been affected by diabetes in 2019[1]. The death ratio and economic costs associated with diabetes and its complications are considerably high[2]. Traditional antidiabetic drugs such as biguanides, insulin, and sulfonylureas have several drawbacks such as short half-lives, oral unavailability or undesirable side effects like hypoglycemia, diarrhea, liver diseases, renal failure, respiratory tract infections, musculoskeletal pain, enlarged urination and urinary tract infections, and weight gain. Recent therapies are directed towards glucose control through glucagon-like peptide-1 (GLP-1) receptor agonists, DPP-IV inhibitors and sodium-glucose co-transporter 2 (SGLT2) inhibitors to overcome these shortcomings[3,4].

Dipeptidyl peptidase-IV (DPP-IV) enzyme is a member of a family of serine peptidases that includes quiescent cell proline dipeptidase (QPP), DPP-VIII and DPP-IX. The DPP-IV enzyme is a key regulator of incretin hormones. The DPP-IV inhibitors competitively inhibit the enzyme. This enzyme breaks down the incretins – GLP-1 (glucagon-like peptide-1) and GIP (glucose-dependent insulinotropic polypeptide), gastrointestinal hormones that are released in response to a meal[5]. By preventing GLP-1 and GIP inactivation, GLP-1 and GIP are able to potentiate the secretion of insulin and suppress the release of glucagon by the pancreas. This drives blood glucose levels towards normal[6].

Sitagliptin, vildagliptin, saxagliptin, linagliptin, trelagliptin, omarigliptin and alogliptin are the well-known approved DPP-IV inhibitors. Amongst these, trelagliptin and omarigliptin were having once-weekly dosing regimen. Although patient satisfaction and compliance have been increased, fewer adverse effects like renal and hepatic function impairments have still been observed in clinical study of omarigliptin[7]. Some adverse effects are also found with other approved DPP-IV inhibitors like vildagliptin (headache), saxagliptin (nasopharyngitis), and sitagliptin (pancreatitis)[8]. By exploring the design and development of structurally diversified DPP-IV inhibitors with long acting antidiabetic efficacy, such issues can be addressed. Computer aided drug design (CADD) tools can provide the important platform for designing novel DPP-IV inhibitors.

In the present study, we executed CADD tools like Three-Dimensional Quantitative Structure-Activity Relationship (3D-QSAR) pharmacophore modeling and virtual screening.

Based on virtual screening, we have designed, synthesized, and screened some aminal derivatives to evaluate their antidiabetic potentials.

Experimental

Computational studies:

Materials and methods:

The 3D-QSAR pharmacophore modeling studies were performed using Discovery Studio 2.1 (DS) software package (Accelrys Inc.).

Selection of the training set:

A set comprising of 56 compounds having DPP-IV inhibitory activity was taken from the available literatures and was used in the present study[9–11]. The selected compounds for the dataset evaluated by same bioassay method, similar species and similar tissue. Several moderately active and inactive compounds were also being included in order to cover all magnitude of order of activity. The compounds are divided into training and test set as described below. For generation of pharmacophore model using *HypoGen*, selection of training set is very important.

Important requirements for the selection of training set are[12]:

(a) The minimum number of molecules in *HypoGen* algorithm is 16.

(b) The activity data should be in 5–6 orders of magnitude.

(c) The most active compounds should be included.

Out of 46 compounds, 20 compounds with enzyme inhibitory activity ranging from 0.003 to 170 μM spanning six orders of magnitude were taken as training set (Table S1) and the remaining 26 compounds were taken as test set. The enzyme inhibitory activity for test set were ranging from 0.009 to 47 μM (Table S2).

Compound preparation and conformation generation:

The 3D structures of all the compounds in this study were drawn using Visualizer module of Accelrys Discovery Studio 2.1 (DS). The CHARMm force field was used for calculation of potential energy. Energy minimization of all compounds were done using smart minimizer method, which uses steepest descent method, followed by the conjugate gradient method for faster convergence towards a local minimum, until the root mean square gradient value becomes smaller than 0.001 kcal/mol, followed by geometry optimization by semi-empirical *MOPAC-AM1* method[13].

There are three types of conformational analysis: FAST analysis, BEST analysis and CAESAR analysis. In this work, BEST quality conformer generation method was set 255, the maximum number, with an energy range of 20 kcal/mol above the estimated global minimum for each molecule. All other parameters used were kept same at their default setting.

3D-QSAR pharmacophore model generation:

The 3D-QSAR pharmacophore method uses the chemical features of most active and inactive compounds along with their biological activity. In this study, we applied the 3D-QSAR-based pharmacophore method for generation of pharmacophore models which can be used to evaluate the activity of newly designed compounds. *Feature mapping* protocol of Discovery Studio was used to distinguish the features that are present in the training set compounds. Each feature is defined by a chemical function, location and orientation in 3D space, tolerance in location, and weight. *HypoGen* pharmacophore model generation process was performed[14]. It allows maximum five features from a set of eleven features which are hydrophobic (HY), hydrogen bond acceptor (HBA), hydrogen bond acceptor lipid (HBAL), hydrogen bond donor (HBD), hydrophobic aliphatic (HYAl), hydrophobic aromatic (HYAr), positively (PC) and negatively (NC) charged, positively (PI) and negatively (NI) ionizable, and ring aromatic (RA).

Taking into account the chemical features of the compounds included in the training set, three features were selected in the hypothesis generation: hydrogen bond acceptor (HBA), hydrogen bond donor (HBD), and hydrophobe (HY). The generated pharmacophore was of three features and four points, which contains one HBA, one HBD, and two HY. The best hypothesis was hypothesis-1 shown in Table 1. The best pharmacophore model was selected based on the large cost difference, high correlation coefficient (r^2), and lower RMSD.

Validation of pharmacophore hypothesis:

The selected pharmacophore model was validated using three methods: Cost analysis, Fischer's randomization test, and test set prediction. A larger difference between the fixed and null costs than that between the fixed and total costs signifies the quality of a pharmacophore model. The total

cost of any pharmacophore hypothesis should be close to the fixed cost to provide any useful models[15]. For generated Hypo 1 model, the cost difference was 51.75 and configuration cost was 11.78. These values suggested that the generated model was comparatively better. Fischer randomization is another approach for pharmacophore model validation. The 95% confidence level was selected in this validation study and 19 random spreadsheets were constructed. This validation method checks the correlation between the chemical structures and biological activity. This method generates pharmacophore models using the same parameters as those used to develop the original pharmacophore model by randomizing the activity data of the training set compounds. At last, test set validation was performed. All the compounds included in test set were mapped on the best hypothesis (Hypo 1) with the help of ligand mapping feature given in protocol.

The chemical database of diversified chemical structures was screened for pharmacophore-based virtual screening. The molecules having highest fit values were selected for synthesis and evaluated for DPP-IV inhibition.

Chemistry:

All the reagents and solvents required for the synthesis of the compounds were procured from Sigma-Aldrich, Spectrochem, and S. d. fine chemicals. Reaction monitoring was carried out by thin-layer chromatography (TLC), using silica gel precoated plates ($60F_{254}$, Merck, 0.25 mm thickness) and visualized in ultraviolet (UV) light (λ = 254 nm) or in an iodine chamber. Melting points were determined in glass capillary tubes using a silicon oil-bath type melting point apparatus (Veego) and the reported melting points are uncorrected. The IR spectra were recorded on in FT-IR 8400S Shimadzu spectrophotometer using KBr. Mass spectra were obtained using 2010EV LCMS Shimadzu instrument at 70 eV. ^{1}H NMR spectra were recorded in DMSO-d_6 on BRUKER Avance-II at 400 MHz and chemical shift were measured as parts per million downfield from tetramethylsilane (TMS) as internal standard.

*Ethyl 2-cyano-3,3-bis(methylthio)acrylate (**3**):*

To a stirred solution of potassium hydroxide (13.2 g, 0.2 mol) in water (10 mL), ethyl cyanoacetate (11.3 g, 0.1 mol) and DMF (15 mL) at 0°C was dropwise added carbon disulfide (7.6 g, 0.1 mol) and the mixture was stirred further for 1 h. Then the reaction mixture was treated dropwise with dimethyl sulphate (25.2 g, 0.2 mol) maintaining the temperature at 0–5°C. The mixture was allowed to stand at room temperature for 24 h. The reaction mixture was poured into ice water. The resulting suspension was filtered, washed with water, and dried to obtain yellow colored compound. The crude product was crystallized using *n*-hexane to obtain the titled compound (18.4 g, 85%), yellow solid, m.p. 57–59°C (lit.[16] m.p. 58–60°C).

*N-Benzyl-2-cyano-3,3-bis(methylthio)acrylamide (**4**):*

The use of *N*-benzylcyanoacetamide in place of ethyl cyanoacetate following the same procedure as described for the preparation of **3**, the title compound **4** was obtained as yellow solid (6.2 g, 78%), m.p. 83–86°C (lit.[17] m.p. 85–86°C).

*General procedure for the synthesis of 3-(substituted amino)-2-(substituted)-(methylthio)]acrylonitrile (S,N-acetals) (**5-8**):*

Method A[18]: To a stirred solution of 2-substituted-3,3-bis(methylthio)acrylonitrile (**3**/**4**, 1 g) in ethanol (10 mL) was added the substituted aromatic amines (1.0 equiv.). The reaction mixture was heated under reflux till completion of the reaction as monitored by TLC. The reaction mixture was poured into ice-cold water with vigorous stirring. The solid product was filtered, washed with water, dried, and recrystallized using *n*-hexane.

*Ethyl 2-cyano-3-((2-methoxyphenyl)amino)-3-(methylthio) acrylate (**5**):*

The title compound (**5**) was synthesized from compound (**3**) (1 g, 0.0046 mol) and *o*-anisidine (0.56 g, 0.0046 mol) following **Method A** (yield: 1.17 g, 90%). Brown solid; m.p. 99–103°C (lit.[19] m.p. 101–102°C); IR (KBr, cm^{-1}): 3169 (-NH), 2940 (C-H, aromatic), 2210 (-C≡N), 1652 (C=O, ketone).

*N-Benzyl-2-cyano-3-((2-methoxyphenyl)amino)-3-(methylthio)acrylamide (**6**):*

The title compound (**6**) was synthesized from compound (**4**) (1 g, 0.0035 mol) and *o*-anisidine (0.44 g, 0.0035 mol) following **Method A** (yield: 1.09 g, 87%). White solid; m.p. 128–130°C; IR (KBr, cm^{-1}): 3182 (-NH), 2920 (C-H, aromatic), 2210 (-C≡N), 1620 (C=O, ketone); MS (*m/z*): 354.2 [M+H]$^+$.

*Ethyl 2-cyano-3-((4-hydroxyphenyl)amino)-3-(methylthio) acrylate (**7**):*

The title compound **(7)** was synthesized from compound

(**3**) (1 g, 0.0046 mol) and *p*-aminophenol (0.5 g, 0.0046 mol) following **Method A** (yield: 1.01 g, 79%). Yellow solid; m.p. 113–116°C; IR (KBr, cm^{-1}): 3380 (O-H), 3298 (-NH), 2981 (C-H, aromatic), 2200 (-C≡N), 1660 (C=O, ketone).

*N-Benzyl-2-cyano-3-((3-methoxyphenyl)amino)-3-(methylthio)acrylamide (**8**):*

The title compound **(8)** was synthesized from compound (**4**) (1 g, 0.0035 mol) and *m*-anisidine (0.44 g, 0.0035 mol) following **Method A** (yield: 1.07 g, 95%). White solid; m.p. 132–133°C; IR (KBr, cm^{-1}): 3177 (-NH), 2931 (C-H, aromatic), 2203 (-C≡N), 1626 (C=O, ketone); MS (*m/z*): 354.2 $[M+H]^+$.

*General procedure for the synthesis of 2-(substituted)-3,3-(disubstituted amino)acrylonitrile (Aminals) (**9-12**):*

Method B[18]**:** To a stirred solution of 3-(substituted amino)-2-(substituted)-(methylthio)]acrylonitrile (**5-8**, 1 g) in ethanol (10 mL) was added aqueous ammonia solution (1.0 equiv.). The reaction mixture was heated under reflux till completion of the reaction as judged by TLC. The reaction mixture was poured into ice-cold water with vigorous stirring. The solid product was filtered, washed with water, dried, and recrystallized using *n*-hexane.

*Ethyl 3-amino-2-cyano-3-((2-methoxyphenyl)amino)acrylate (**9**):*

The title compound **(9)** was synthesized from compound (**5**) (1 g, 0.0034 mol) following **Method B** (yield: 0.63 g, 71%). White solid; m.p. 218–220°C; IR (KBr, cm^{-1}): 3387–3380 (NH_2), 3169 (-NH), 2940 (C-H, aromatic), 2210 (-C≡N), 1652 (C=O, ketone); ^{1}H NMR (DMSO-d_6): δ 10.46 (s, 1H, ArN*H*), 9.40 (s, 1H, O*H*), 7.04 (d, 2H, Ar*H*), 6.86 (d, 2H, Ar*H*), 6.13 (s, 2H, NH_2), 4.15 (q, 2H, CH_2CH$_3$), 1.28 (t, 3H, CH$_2$*CH$_3$*); MS (*m/z*): 262.1 $[M+H]^+$.

*3-Amino-N-benzyl-2-cyano-3-((2-methoxyphenyl)amino) acrylamide (**10**):*

The title compound **(10)** was synthesized from compound (**6**) (1 g, 0.0028 mol) following **Method B** (yield: 0.6 g, 66%). White solid; m.p. 197–199°C; IR (KBr, cm^{-1}): 3378–3370 (NH_2), 3182 (-NH), 2920 (C-H, aromatic), 2210 (-C≡N), 1620 (C=O, ketone); ^{1}H NMR (DMSO-d_6): δ 9.52 (s, 1H, ArN*H*), 8.54 (s, 2H, NH_2), 8.04 (t, 1H, CON*H*), 7.23–7.18 (m, 5H, Ar*H*), 6.93–6.61 (m, 4H, Ar*H*), 4.32 (d, 2H, CH_2), 3.86 (s, 3H, OCH_3); MS (*m/z*): 323.1 $[M+H]^+$.

*Ethyl 3-amino-2-cyano-3-((4-hydroxyphenyl)amino)acrylate (**11**):*

The title compound **(11)** was synthesized from compound (**7**) (1 g, 0.0035 mol) following **Method B** (yield: 0.64 g, 73%). White solid; m.p. 234–236°C; IR (KBr, cm^{-1}): 3390 (O-H), 3368–3363 (NH_2), 3298 (-NH), 2981 (C-H, aromatic), 2200 (-C≡N), 1660 (C=O, ketone); ^{1}H NMR (DMSO-d_6): δ 10.42 (s, 1H, ArN*H*), 9.45 (s, 2H, NH_2), 7.02 (d, 2H, Ar*H*), 6.89 (d, 2H, Ar*H*), 6.16 (s, 1H, O*H*), 4.17 (q, 2H, CH_2CH$_3$), 1.31 (t, 3H, CH$_2$*CH$_3$*); MS (*m/z*): 237.9 $[M+H]^+$.

*3-Amino-N-benzyl-2-cyano-3-((3-methoxyphenyl)amino) acrylamide (**12**):*

The title compound **(12)** was synthesized from compound (**8**) (1 g, 0.0028 mol) following **Method B** (yield: 0.57 g, 63%). White solid; m.p. 199–202°C; IR (KBr, cm^{-1}): 3364–3359 (NH_2), 3177 (-NH), 2931 (C-H, aromatic), 2203 (-C≡N), 1626 (C=O, ketone); ^{1}H NMR (DMSO-d_6): δ 9.56 (s, 1H, ArN*H*), 8.58 (s, 2H, NH_2), 8.08 (t, 1H, CON*H*), 7.32–7.26 (m, 5H, Ar*H*), 7.12 (t, 1H, Ar*H*), 6.31 (d, 1H, Ar*H*), 6.21 (m, 1H, Ar*H*), 6.02 (d, 1H, Ar*H*), 4.36 (d, 2H, CH_2), 3.89 (s, 3H, OCH_3); MS (*m/z*): 323.1 $[M+H]^+$.

Biology:

In vitro assay for DPP-IV inhibition[20]*:*

In this study, evaluation of DPP-IV inhibitory activity was performed in 96-well microplates measuring the increase in absorbance at 410 nm using Gly-Pro-p-nitroanilide as DPP-IV substrate. All the experiments were performed in 50 mM Tris-HCl buffer (pH 8). Five different concentrations (0.001–100 μM) of each test compound were used to determine the enzyme inhibition activity. 10 μL of test compounds **(9-12)** were taken, followed by addition of 0.1 mL assay buffer, 0.1 μL enzyme was added, reaction incubation was set for 10 min at 37°C, followed by addition of 10 μL substrate in tris buffer. The reaction was stopped by adding 1 μL HCl. Within one hour after termination of the reaction, the absorbance at 410 nm was observed.

Results and discussion

Computational studies:

Pharmacophore generation:

Ten pharmacophore models were generated using a training set containing 20 compounds using *Feature Mapping*

protocol. All the generated pharmacophore models were composed of either HBA or HBD or both with HY features. The total cost values of ten pharmacophore models were ranged from 92.51 to 104.13 (Table 1). The cost difference between the total cost and null cost must be greater and it should be smaller between total cost and fixed cost values for a significant pharmacophore model. In our study, the pharmacophore generation run calculated a fixed cost value of 80.18 and the null cost value of 144.27. When compared to the total cost values of generated ten pharmacophore models, first model (Hypo 1) has scored the value closer to the fixed cost. The cost difference between the null cost and total cost value of the first pharmacophore model is 51.75. The cost difference value between 40 and 60 implies that the pharmacophore model correlates the experimental and estimated activity values more than 90%. The Hypo 1 was made of four pharmacophoric features consisting one HBA, one HBD and two HY features (Fig. 2). The interfeature distance in Å has been provided in Table 2. The Hypo 1 showed the highest correlation coefficient value of 0.93, which highlighted its strong predictive ability. The RMSD value of 1.03 also supported its good predictivity.

Table 1. Statistical results of the top 10 pharmacophore hypotheses generated by *HypoGen* algorithm

Hypothesis	Total cost	Cost difference[a]	RMSD[b]	Correlation (r^2)	Error cost
Hypo 1	**92.51**	**51.75**	**1.03**	**0.93**	**77.98**
Hypo 2	96.32	47.95	1.20	0.90	81.70
Hypo 3	99.46	44.81	1.18	0.90	81.39
Hypo 4	100.65	43.62	1.21	0.90	82.07
Hypo 5	101.30	42.97	1.21	0.90	82.02
Hypo 6	102.06	42.20	1.27	0.88	83.54
Hypo 7	102.58	41.69	1.32	0.87	84.89
Hypo 8	103.36	40.90	1.30	0.88	84.29
Hypo 9	103.58	40.69	1.33	0.87	85.06
Hypo 10	104.13	40.14	1.32	0.88	84.72

Null cost of total 10 hypotheses = 144.27; fixed cost = 80.18; configuration cost = 11.78; pharmacophore features of Hypo 1 = HBA, HBD, HY, HY.

[a]Cost difference = Null cost – Total cost. [b]RMSD = route mean square deviation.

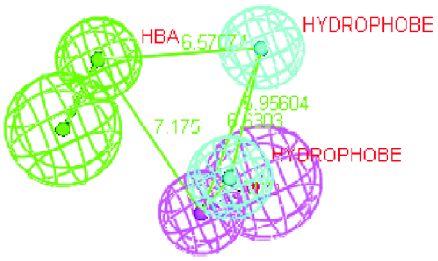

Fig. 1. The best *HypoGen* pharmacophore model, Hypo 1. Green color represents HBA, magenta color represents HBD and cyan color represents HY features.

Table 2. Pharmacophoric features with its interfeature distance

Feature	Feature	Interfeature distance (in Å)
HBA	HBD	7.17
HBA	HY 1	6.57
HBD	HY 1	6.63
HY 1	HY 2	5.95

Pharmacophore validation:

Fischer's randomization test:

The Hypo 1 was validated using Fischer randomization test to check that the model is not resulted due to the random correlation. The purpose of Fischer randomization test is to validate the strong correlation between chemical structures and biological activity. The experimental activities of the training set were scrambled randomly and the resulting training set was used in *HypoGen* with the parameters chosen for the original pharmacophore generation. A set of 19 random spreadsheets was generated to achieve a 95% confidence level that the best pharmacophore Hypo 1 was not generated by chance. None of the randomly generated pharmacophore models during Fischer randomization test has scored better statistical parameters than Hypo 1. The total cost of Hypo 1 (92.90) was close to the fixed cost (80.18). No other randomized test was so closed to it. Highest correlation coefficient was also observed in Hypo 1 than the other randomized trials (Table 3).

Test set validation:

Test set validation is external validation method. In addition to validate the predictive ability of training set molecules; the pharmacophore model should also estimate the activity of new hits.

For test validation all compounds included in test set (26)

Table 3. Results from cross-validation run using Fischer's randomization test

Validation No.	Correlation (r^2)	Total cost
Original hypothesis		
Hypo 1	**0.93**	**92.90**
Randomized hypotheses		
Trial 1	0.45	142.53
Trial 2	0.69	125.40
Trial 3	0.66	125.17
Trial 4	0.69	125.60
Trial 5	0.67	124.86
Trial 6	0.64	132.43
Trial 7	0.72	119.22
Trial 8	0.70	129.27
Trial 9	0.67	125.13
Trial 10	0.77	121.27
Trial 11	0.57	133.35
Trial 12	0.73	115.61
Trail 13	0.75	116.55
Trail 14	0.60	133.29
Trial 15	0.62	130.31
Trial 16	0.48	140.22
Trial 17	0.80	116.95
Trial 18	0.60	130.37
Trial 19	0.68	124.54

were mapped on best hypothesis (Hypo 1) with help of *ligand mapping* feature given in protocol. At the end of success of ligand mapping feature gave estimated activity of all test set compounds, all the compounds were classified on the bases of their activity scale, as highly active compounds (less than 1 μM, denoted by +++), moderately active compounds (1–100 μM, denoted by ++) and/or inactive compounds (100 μM, denoted by +), for both actual and estimated activity. Fit value has also been given for all compounds here.

As shown in Table 4, most of the highly active compounds predicted correctly, only two moderately active compounds were predicted inactive and fourteen highly active compounds were predicted moderately active.

Virtual screening:

To identify novel and potent DPP-IV inhibitors, virtual screening was performed using the best flexible database search tool in catalyst program. The best pharmacophore model (Hypo 1) was used as a query to search a manually generated in house database. A database search was done using *ligand pharmacophore mapping* which involves two fitting methods: rigid fitting performs rigid fit between ligand and pharmacophore and flexible method performs flexible fit between ligand and pharmacophore

Table 4. Experimental and estimated IC_{50} values of the training set compounds based on best pharmacophore hypothesis Hypo 1

Compound No.	Experimental IC_{50} (μM)	Estimated IC_{50} (μM)	Fit value[a]	Experimental activity scale	Estimated activity scale
A21	0.009	0.001	9.66	+++	+++
A22	0.0013	0.001	9.47	+++	+++
A23	0.0017	0.002	9.25	+++	+++
A24	0.0011	0.001	9.71	+++	+++
A25	0.01	34.579	4.98	+++	++
A26	0.011	41.851	4.89	+++	++
A27	0.024	42.414	4.92	+++	++
A28	0.047	30.767	5.05	+++	++
A29	0.09	48.859	4.83	+++	++
A30	0.013	0.001	9.49	+++	+++
A31	0.27	55.102	4.77	+++	++
A32	0.24	45.689	4.86	+++	++
A33	0.34	37.948	4.94	+++	++
A34	0.13	37.571	4.94	+++	++
A35	0.18	62.394	4.77	+++	++
A36	0.18	54.558	4.78	+++	++
A37	1	5.532	4.68	++	++

Table-4 (contd.)

A38	1.4	5.894	4.33	++	++
A39	1.5	241.616	4.71	++	+
A40	1.5	6.009	5.74	++	++
A41	1.75	25.251	5.11	+++	++
A42	2.5	64.372	4.72	++	++
A43	14	13.036	5.40	++	++
A44	18	16.760	6.94	++	++
A45	20	75.568	0.64	++	+
A46	47	43.762	18.14	++	++

[a]Fit value indicates how well the features in the pharmacophore map the chemical features in the compound.

[b]Activity scale: IC_{50} < 1 μM (Most active, +++); 1–100 μM (Active, ++); >1000 μM (Inactive, +).

We have used here flexible search method. In the present study, best flexible conformation generation was used to find out the hit from manually generated database. The structures of only potent compounds obtained from virtual screening were shown in Table 5 with estimate activity and fit value.

Pharmacophore mapping of compounds mentioned in Sr. no. 2 and 3 in Table 5 were carried out using best pharmacophore model (Hypo 1) (Fig. 2A and 2B).

Chemistry:

The synthesis of the *N*,*N*-acetal derivatives (Aminals) **(9-12)** is as depicted in Scheme 1.

The whole procedure is comprised of three synthetic steps. The general method for preparation of ethyl 2-(substituted)-3,3-bis-(methylthio)acrylonitrile (*S*,*S*-acetals) **(3** and **4)** involved the condensation of the active methylene compound (e.g. ethyl cyanoacetate, cyanoacetamide, malononitrile etc.) with carbon disulphide in the presence of potassium hydroxide followed by alkylation of the dithiolate anion with dimethylsulphate (DMS). The 2-(substituted)-3-(substituted amino)-3-(methylthio)acrylonitriles (*S*,*N*-acetals) **(5-8)** were obtained by nucleophilic displacement of one thiomethyl

Table 5. List of predicted molecules based on virtual screening

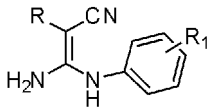

Sr. No.	R	R_1	Estimated IC_{50} (μM)	Fit value
1*	-OCOEt	2-OMe	0.025	8.087
2*	-CONHBn	2-OMe	0.009	8.578
3*	-OCOEt	4-OH	0.019	8.232
4*	-CONHBn	3-OMe	0.009	8.578
5	-OCOEt	3-OH	0.076	7.939
6	-OCOEt	4-OMe	0.099	7.822
7	-OCOEt	3-OMe	0.032	8.015
8	-OCOEt	4-Cl	0.146	7.753
9	-OCOEt	4-Me	0.379	7.576
10	-CONHBn	4-OH	0.012	8.362

*Top for compounds having highest estimated IC_{50} values were chosen for the synthesis.

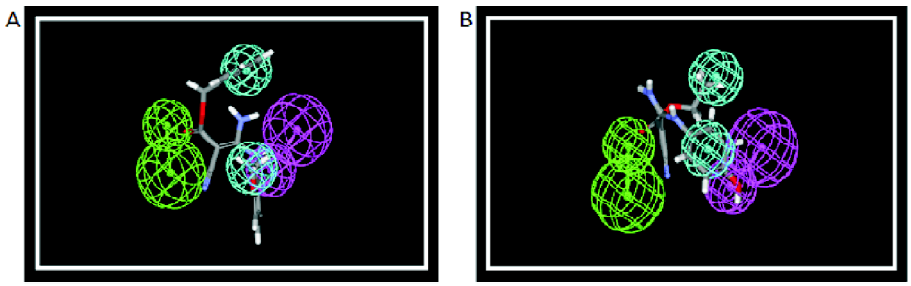

Fig. 2. Pharmacophore mapping of predicted compounds (A) (shown in Sr. no. 2 of Table 5), (B) (shown in Sr. no. 3 of Table 5). Green color represents HBA, magenta color represents HBD and cyan color represents HY features.

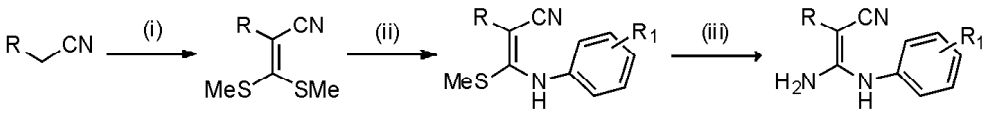

1, 2 **3, 4** **5-8** **9-12**

Compd	R
1, 3	-OCOEt
2, 4	-CONHBn

Compd	R	R_1
5, 9	-OCOEt	2-OMe
6, 10	-CONHBn	2-OMe
7, 11	-OCOEt	4-OH
8, 12	-CONHBn	3-OMe

Scheme 1. Synthetic route for the synthesis of compounds **(9-12)**. Reagents and conditions: (i) KOH, CS_2, DMS, DMF, 0–5°C, (ii) $ArNH_2$, ethanol, reflux and (iii) aqueous NH_3, ethanol, reflux.

group of the 2-(substituted)-3,3-bis(methylthio)acrylonitrile **(3,4)** by various substituted aromatic amines. [3,3-(Disubstituted amino)-2-(substituted)]acrylonitriles (*N*,*N*-acetals, Aminals) **(9-12)** were obtained by nucleophilic displacement of thiomethyl group of the 2-(substituted)-3-(substituted amino)-3-(methylthio)acrylonitriles (*S*,*N*-acetals) **(5-8)** by ammonia.

Biological evaluation:

DPP-IV inhibitory studies:

The obtained novel Aminal derivatives **(9-12)** were evaluated for their DPP-IV inhibitory activity. The obtained IC_{50} values of compounds were shown in Table 6.

Table 6. *In vitro* DPP-IV inhibitory activities of synthesized compounds **(9-12)**

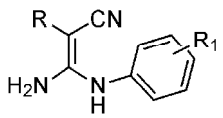

9-12

Compound No.	R	R_1	IC_{50} (μg/mL)
9	-OCOEt	2-OMe	0.122
10	-CONHBn	2-OMe	0.08
11	-OCOEt	4-OH	0.078
12	-CONHBn	3-OMe	0.073

All four compounds **(9-12)** showed good DPP-IV inhibition at different concentrations.

For checking the correctness of the model (Hypo 1), comparison between observed and predicted IC_{50} values were carried out as shown in Table 7. When error values are less than ±100, it is considered to be good. All the compound showed very less error, so these compounds are considered as potent DPP-IV inhibitors. Amongst these four compounds, compound **(9)** seemed to be best correlated with the computational and experiment data as it showed least error. Compound (**10)** and (**12)** proved to be potent DPP-IV inhibitors as they have shown the least IC_{50} values.

Table 7. Comparison of observed and predicted enzyme inhibitory activity of synthesized compounds **(9-12)**

Compound No.	Observed IC_{50} (μM)	Predicted IC_{50} (μM)	Error
9	0.035	0.025	1
10	0.248	0.009	23.1
11	0.312	0.019	29.1
12	0.226	0.009	21.7

Conversion of IC_{50} values from mg/mL into mM: By dividing μg/mL with molecular weight of compound and multiplying it with 1000.

Conclusions

In the present study, a 3D-QSAR-based pharmacophore model, Hypo 1, was developed with one HBD, one HBA and two HY features, having 0.93 correlation coefficient. The validation of generated hypothesis was carried out using cost analysis (cost difference = 51.75; configuration cost = 11.78)

and Fischer randomization test. The predictive ability of generated hypothesis was also checked using a set of 26 test compounds. Result showed that majority of compounds were predicted correctively with lower error value and good fit value. The best hypothesis (Hypo 1) was used as 3D query for searching the manually generated in house database which identified structurally diverse scaffold with predicted activity ranges from 0.005–0.5 μM as plausible leads for designing novel DPP-IV inhibitors. Compounds **9**, **10**, **11**, and **12** were synthesized and screened for DPP-IV inhibitory activity on human serum. All the compounds were found to be potent suggesting error values comparatively less. Activity of synthesized compounds was found nearly comparable to that of predicted one which suggests that the generated pharmacophore model has good predictive power.

Acknowledgements

The authors acknowledge Oxygen Healthcare Research Pvt. Ltd., Ahmedabad for carrying out Mass analysis and SAIF, Punjab University, Chandigarh for carrying out NMR analysis.

References

1. International Diabetes Federation, https://www.idf.org/, accessed on 11th July, 2020.
2. W. H. Polonsky and R. R. Henry, *Patient Prefer. Adherence*, 2016, **10**, 1299.
3. M. Guo, J. Gu. F Teng, J. Chen, X. Ma, Q. Chen, Y. Pu, Z. Jiang, Y. Long and Y. Xu, *Endocrine*, 2020, **67**, 294.
4. P. Timmins, S. S. Hasan and Z. Babar, *Prim. Care Diabetes,* 2019, **13**, 409.
5. N. Lia, L. Wang, B. Jiang, S. J. Guo, X. Q. Lia, X. C. Chen, J. Luo, C. Lia, Y. Wange and D. Y. Shia, *Bioorg. Med. Chem. Lett.*, 2018, **28**, 2131.
6. B. D. Patel, S. V. Bhadad and M. D. Ghate, *Bioorg. Chem.,* 2017, **72**, 345.
7. A. Musoev, S. Numonov, Z. You and H. Gao, *Molecules,* 2019, **24**, 2870.
8. K. G. Seshadri and M. H. B. Kirubha, *Indian J. Pharm. Sci.,* 2009, **71(6)**, 608.
9. J. Peters, D. Hunziker, H. Fischer, M. Kansy, S. Weber, S. Kritter, A. Muller, A. Wallier, F. Ricklin, M. Boehringer, S. M. Poli, M. Csato and B. M. Loeffler, *Bioorg. Med. Chem. Lett.,* 2004, **14(13)**, 3575.
10. A. Lozama and T. E. Prisinzaro, *Bioorg. Med. Chem. Lett.,* 2011, **19(18)**, 5490.
11. J. Deng, L. Peng, G. Zhang, X. Lan, L. C. Li, F. Chen, Y. Zhou, Z. Lin, L. Chen, R. Dai, H. Xu, L. Yang, X. Zhang and W. Hu, *Eur. J. Med. Chem.,* 2011, **46(1)**, 71.
12. E. M. Krovat and T. Langer, *J. Med. Chem.,* 2003, **46**, 716.
13. O. Gürsoy and M. Smieško, *J. Cheminform.,* 2017, **9**, 29.
14. S. John, S. Thangapandian, M. Arooj, J. C. Hong, K. D. Kim and K. W. Lee, *BMC Bioinformatics,* 2011, **12**, 1.
15. R. Sarma, S. Sinha, M. Ravikumar, M. K. Kumar and S. K. Mahmood, *Eur. J. Med. Chem.,* 2008, **43**, 2870.
16. H. Junjappa and C. V. Asokam, *Tetrahedron Lett.*, 1990, **46(15)**, 5423.
17. N. Long, X. J. Cai, B. A. Song, S. Yang, Z. Chen, P. S. Bhadury, D. Y. Hu, L. H. Jin and W. Xue, *J. Agric. Food Chem.,* 2008, **56(13)**, 5242.
18. S. Makwana and H. Rabari, *Pharma Sci. Monit.*, 2017, **8(3)**, 328.
19. V. S. Bhadti, Studies on the synthesis of pyrimidines from ketene thioacetals and condensed pyrimidines from *o*-aminonitriles by the reaction with nitriles under acidic conditions, PhD thesis, Gujarat University, 1985, 106.
20. S. Schape, I. D. Meester, G. Vanhoof, D. Hendriks, M. V. Sande, K. V. Camp and A. Yaron, *Clin. Chem.*, 1988, **34(11)**, 2299.